PHYSICAL REVIEW E **84**, 060701(R) (2011)

Short-range correlations seen in the nematic phase of bent-core liquid crystals by dielectric and electro-optic studies

Yun Jang,[1] Vitaly P. Panov,[1] A. Kocot,[1,2] A. Lehmann,[3] C. Tschierske,[3] and J. K. Vij[1,*]
[1]*Department of Electronic and Electrical Engineering, Trinity College Dublin, Dublin 2, Ireland*
[2]*Institute of Physics, Silesian University, Katowice, Poland*
[3]*Institute of Organic Chemistry, Martin Luther-University Halle-Wittenberg, D-06120 Halle/Saale, Germany*
(Received 18 August 2011; published 19 December 2011)

Three bent-core nematic liquid crystals having the same core but with different terminal groups, short (C4) and long (C7,C9) tails, are investigated by dielectric and electro-optic contrast spectroscopic techniques. C4 shows sign reversal in the dielectric anisotropy $\Delta\epsilon'$ as a function of both temperature and frequency, whereas C9 shows only negative $\Delta\epsilon'$ in the entire mesophasic region. The behavior of C7 is intermediate of the two. Results of a dielectric study show that both C7 and C9 exhibit strong short-range polar correlations normal to the director. The correlation lengths of these interactions are found to be similar to those from the x-ray scattering. An increased hindered rotation for C9 compared to C4 moves the dielectric dispersion for $\epsilon'_{\parallel}$ to much lower frequencies, such that C9 shows only negative $\Delta\epsilon'$ over the entire temperature range.

DOI: 10.1103/PhysRevE.84.060701 PACS number(s): 61.30.Eb, 42.70.Df, 77.22.Ch

The molecular structure of a liquid-crystalline compound has been found to have a significant influence on its properties and the phase behavior. The typical structure of a calamitic mesogen consists of a rigid core having a couple of phenyl rings and one or two flexible terminal chains. The anisotropic properties of the core moiety plays a key role in the formation of the orientational order of liquid-crystalline (LC) phases, while the terminal chains stabilize positional order, reduce the melting points and extend the phase ranges. The bent-core or banana-shaped mesogens give rise to special kind of nematic phases, in addition to the well-known B1 to B8 phases [1,2], and during the past few years the isotropic-to-nematic (*I*-*N*) transition temperature has been consistently lowered and the range of the nematic phase extended [3]. These materials in their nematic phase display unusual physical properties. Some of these are giant flexoelectricity [4], unprecedented electroconvection [5], and splitting in small-angle scattering patterns [6]. The splitting in small x-ray scattering has been interpreted either in terms of a presence of smectic-*C* (Sm*C*)-like nanostructures [7–9] in the nematic phase or in terms of the form factor of the banana system [10,11]. A strong debate about the appropriateness of such an interpretation is continuing [12]. In this Rapid Communication, dielectric and electro-optic spectroscopic studies of the two representatives of cyanoresorcinols, 4-cyanoresorcinols (C4 and C9), specifically are compared. The results of C7, whose behavior is in between the two, are also given [13]. Interestingly we find that C9 exhibits only negative dielectric anisotropy $\Delta\epsilon'$ whereas C4 shows a reversal in $\Delta\epsilon'$ from positive to negative both with temperature and frequency. We later examine in detail the various causes for the observed sign reversal in $\Delta\epsilon'$ given in the recent literature. In contrast, however, we find that the Maier-Meier model, which includes the anisotropic Kirkwood correlation factors [14], explains the observed behavior extremely well. The unusual dielectric behavior of C9 is interpreted in terms of the short-range molecular associations along and normal to the director. These show that such an association exists in both C7 and C9, which is also supported by results from small-angle x-ray diffraction.

Derivatives of 4-cyanoresorcinol bisbenzoates shown in Fig. 1 are synthesized with different chain lengths in the terminal groups [14]. The dielectric spectra for different temperatures are recorded for both homeotropic and planar cells as a function of frequency using a Novocontrol dielectric spectrometer. Dielectric and optical cells are prepared using low-resistance indium tin oxide (ITO) glass substrates (20 $\Omega/\square$); these substrates are further coated with the alignment layer depending on the type of alignment needed for the experiment. The data of $\epsilon'_{\parallel}$ and $\epsilon'_{\perp}$ of the different resorcinols are recorded as a function of frequency and temperature, and these are shown for preselected frequencies of 1 and 100 kHz for C4 and C9 as a function of $T^* = T_{N\text{-}I}/T$ in Fig. 2.

The experimental data of complex permittivity (ϵ' and ϵ'' both for homeotropic and planar cells) are analyzed in terms of the relaxation frequency f_R and the dielectric strength $\delta\epsilon$ for each mode. As an example, the results of C4 are presented in Fig. 3, which will be discussed later. The static permittivities of C4 and C9 in a homeotropic cell close to zero frequency cannot be determined since the latter leads to colossal ϵ' and ϵ'' values arising from double-surface layers as a result of large dc conductivity arising mainly from ions. Due to this limitation of the dielectric technique at low frequencies, the electro-optic contrast spectroscopic [13], which is insensitive to the dc conductivity, is used (Fig. 4). Here the transmittance, color coded in arbitrary transmittance units, is plotted as a function of T^*. A line on the graph implies a contour of constant transmittance. The crowded lines imply a sharp change in the transmittance, i.e., the Freedericksz transition occurs at a frequency below for the sign reversal of $\Delta\epsilon'$ such that the condition $E_{\text{th}} = (\pi/d)\sqrt{K_{11}/\epsilon_0\Delta\epsilon'}$ is satisfied. The crossover frequency of C4 is such that $\epsilon'_{\parallel}$ has already relaxed below 1 kHz, whereas $\epsilon'_{\perp}$ would start relaxing at frequencies higher than 5 kHz. K_{11} is the splay elastic constant.

*jvij@tcd.ie

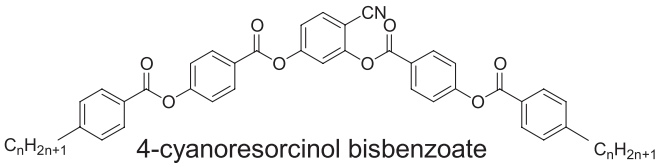

FIG. 1. Chemical structure of 4-cyanoresorcinol bisbenzoates. $n = 4$, C4: I 107 N; $n = 7$, C7: I 111 N_{cybC} 41 Cyb$C$ 25 SmC; $n = 9$, C9: I 104 N_{cybC} 58 Cyb$C$ 50 SmC. N_{cybC} is the nematic phase composed of SmC-type cybotactic clusters and Cyb$C$ is a mesophase composed of elongated cybotactic clusters. The transitions temperatures (T/°C) are obtained during cooling [3].

The total permittivity of a cell configuration is the sum of ϵ_∞ and the various relaxation strengths as given in Fig. 3 for C4, as an example. The static permittivity values for C4, C7, and C9 thus calculated are given in Fig. 5. $\epsilon_\parallel$ and $\epsilon_\perp$ are also calculated from the Maier-Meier (M-M) model by taking the total dipole moment and its transverse and longitudinal components, and the temperature dependence of S determined from the birefringence measurements. The M-M expressions for $\epsilon_\parallel$ and $\epsilon_\perp$ are given as follows [14]:

$$\epsilon_\parallel - \epsilon_{\parallel\infty} = \frac{NhF^2 g_\parallel}{3\epsilon_o k_B T}\left[\mu_l^2(1+2S\rangle + \mu_t^2(1-S)\right], \quad (1)$$

$$\epsilon_\perp - \epsilon_{\perp\infty} = \frac{NhF^2 g_\perp}{3\epsilon_o k_B T}\left[\mu_l^2(1-S) + \mu_t^2\left(1+\frac{1}{2}S\right)\right]. \quad (2)$$

Here μ_l and μ_t are the longitudinal and the transverse components of the molecular dipole moment. $\frac{NhF^2 g_\parallel}{3\epsilon_o k_B T}$ and $\frac{NhF^2 g_\perp}{3\epsilon_o k_B T}$ are the multiplying factors for the permittivities. N is the number density, ϵ_o is the permittivity of vacuum, $k_B T$ is the thermal energy, and F and h are the internal field factors for the reaction and the cavity fields. $g_\parallel$ and $g_\perp$ are the anisotropic Kirkwood correlation factors for the director parallel and perpendicular to the electric field, respectively. For each temperature, $g_\parallel$ and $g_\perp$ are calculated using Eqs. (1) and (2) and by using the experimental values of $\epsilon_\parallel$ and $\epsilon_\perp$ and the scaling factors from C4. This equation was initially introduced to describe the static dielectric properties of sticklike anisotropic systems but, within the limitations of the experiment, it describes

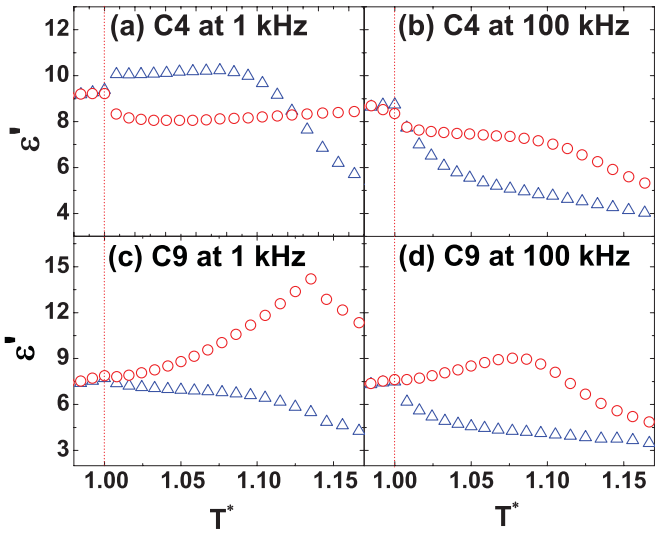

FIG. 2. (Color online) Real part of dielectric permittivity of 4′-resorcinols (C4 and C9) for frequencies of 1 and 100 kHz vs T^*. $\epsilon'_\parallel$, $\epsilon'_\perp$ are shown as blue triangles and red circles, respectively. $T^* = T_{N\text{-}I}/T$. The red dotted vertical line represents the isotropic to the nematic transition temperature.

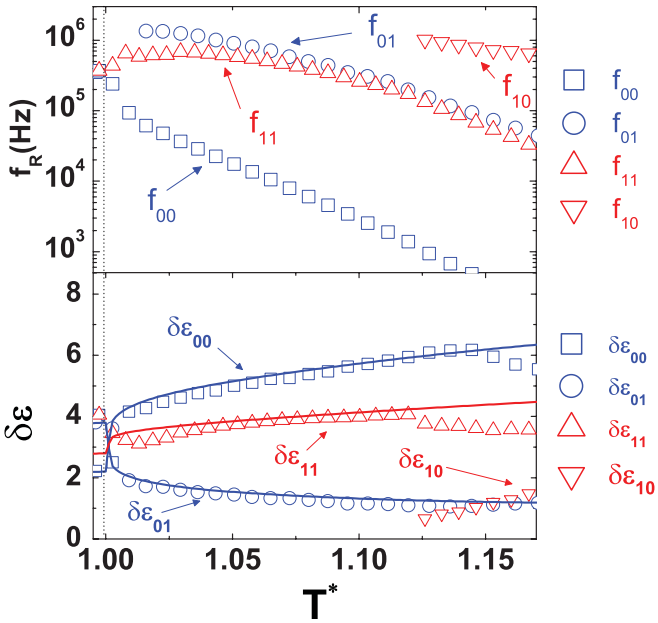

FIG. 3. (Color online) Relaxation frequency $f_{ij} \approx (2\pi\tau_{ij})^{-1}$, and the dielectric strength ($\delta\epsilon_j$) obtained by fitting the measured permittivity data to the Havriliak-Negami equation, for planar (red triangles) and homeotropic cells (blue circles and squares) of C4. f_{ij} and $\delta\epsilon_{ij}$ denote the relaxation frequency and the dielectric strength of the i,jth mode [16]. $T^* = T_{N\text{-}I}/T$. The solid lines indicate a fit to the M-M model. The black vertical dotted line indicates the isotropic-to-nematic transition.

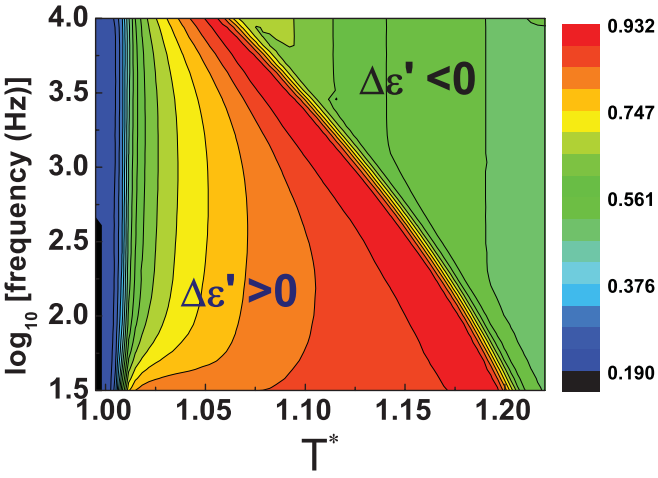

FIG. 4. (Color online) Frequency-temperature plot of the transmittance for C4 in a planar cell of thickness 5 μm and $E = 1.0\,\mathrm{V}/\mu\mathrm{m}$; the color (shade) of the contour represents the transmittance level in arbitrary units. The lines are contours of constant transmittance. The crowded lines imply a sharp change in the transmittance through the cell, that is, a Freedericksz transition occurs due to a sign reversal in $\Delta\epsilon'$ [13].

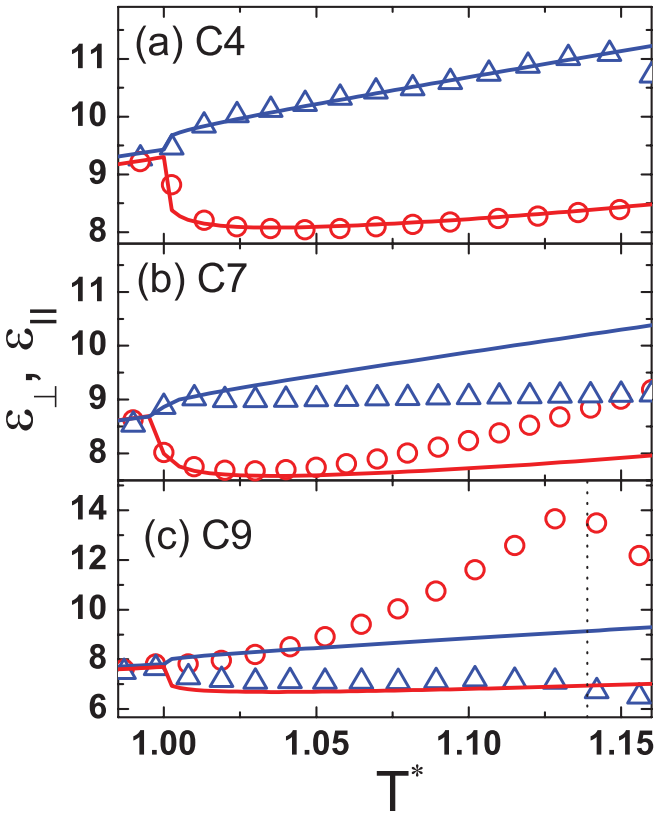

FIG. 5. (Color online) Comparison of static and theoretical permittivities of C4 (a), C7 (b), and C9 (c) using the M-M model (solid lines). The blue triangles and red circles indicate $\epsilon_\parallel$ and $\epsilon_\perp$, respectively. These are calculated by adding dielectric strengths for various processes to ϵ_∞. The blue (dark gray) and red (gray) lines denote calculated values of permittivity with $\mu_l^2/\mu^2 = 0.368$ and $\mu_t^2/\mu^2 = 0.632$, respectively. The vertical dotted line in (c) denotes the transition from $N_{\mathrm{cyb}C}$ to Cyb*C*. We find $\beta = 52.7^\circ$.

such properties of bananalike systems fairly reasonably. The frequency dependencies of $\epsilon'_\parallel$ and $\epsilon'_\perp$ are determined by replacing the orientation parts due to μ_l and μ_t on the right-hand side of Eqs. (1) and (2) by the corresponding spectral densities of the relaxation functions $C_{mn} = \delta\epsilon_{mn}/(1+\omega^2\tau_{mn}^2)$. Here $\delta\epsilon_{mn}$ and τ_{mn} denote the relaxation strength and the relaxation time of the (mn)th mode, respectively. Analytical solutions have been found by Coffey and Kalmykov [16]. The dielectric relaxation strength for a mode will be a part of its scaling factor. A demonstration of the fitting to Eq. (1) is shown in Fig. 3, from which the scaling factors for μ_l and μ_t are obtained. According to these equations, such a reversal in $\Delta\epsilon'$ can be interpreted as arising from the relaxations of the $\epsilon'_\parallel$ and $\epsilon'_\perp$ occurring at different frequencies. f_{00} is retarded while f_{11}, f_{01}, and f_{10} are accelerated due to the nematic order.

A different reason for the sign reversal in a calamitic LC in its nematic phase with a nematic-to-Sm*A* phase transition had been given earlier [17]. The nanosized clusters grow in the nematic phase prior to the transition to the smectic phase due to a pretransitional phenomenon. The small-angle x-ray scattering pattern in the nematic phase of bent-core LCs has been interpreted in terms of such clusters [3]. This cause is ruled out since C4 does not exhibit any strong small-angle x-ray scattering. Another reason for the sign reversal in $\Delta\epsilon'$ that has been advanced in the literature is that of a change in the dipole moment with temperature arising from a conformational change [18,19] caused by the flexibility in the core moiety. However, such a change accompanies a change in the bent angle θ_V and a change in the molecular dipole moment. Such a behavior is normally observed in liquid-crystalline dimers consisting of two rigid meosogenic groups linked by a flexible alkyl chain [20]. But a conformational change should also affect the birefringence, and this is not observed here. If the conformational change is the likely cause, then the angle that the dipole moment makes with the long molecular axis β should change. Based on the ir absorbance measurements of the cyano group, we find that β', the angle that the transition dipole moment makes with the symmetry axis, does not change with reduced temperature. Usually $\beta \simeq \beta'$. If this is the case, then there is no significant change in θ_V and hence in the molecular dipole moment. Thus a conformational change is also ruled out for the sign inversion in $\Delta\epsilon'$.

We find that a sign reversal in $\Delta\epsilon'$ in the nematic phase arises from the relaxation of the longitudinal component of the dipole moment at much lower frequencies than the transverse component. Furthermore, the dielectric strengths for $\epsilon'_\parallel$ are greater than for $\epsilon'_\perp$. This explains the observed behavior of the crossover temperature in $\Delta\epsilon'$ as frequency dependent. The calculation of relaxation times in terms of the nematic potential and S by Saupe is extended by Coffey and Kalmykov [16], who find the exact solutions for the various relaxation times. Each of these permittivities thus shows at least two relaxation modes. The molecular dynamics can be described in terms of four rotational modes f_{00}, f_{01}, f_{10}, and f_{11}. For $\epsilon'_\parallel$ investigated using a homeotropic cell, the modes are (i) the end-over-end rotation f_{00} and (ii) the precessional motion of the long molecular axis around the director of the phase f_{01}. For $\epsilon'_\perp$ investigated using a planar cell, the modes are (iii) the rotation around its own long molecular axis f_{10} and (iv) a combination of precession around the director and the rotation around the long axis f_{11}. The temperature dependence of the dielectric relaxation strength for each component of the dipole moment is primarily determined by the dependence of the principal order parameter S on temperature. We find from Fig. 5 that results for C4 are well reproduced by the M-M model by assuming $g_\parallel = g_\perp = 1$. If this assumption is adopted, the results between the theory and experiment for C9 disagree. The only simple appropriate explanation for this disagreement is that both g values are not equal to unity. $g_\parallel$ and $g_\perp$ are calculated for each temperature with Eqs. (1) and (2) and the experimental values of $\epsilon_\parallel$ and $\epsilon_\perp$ and the appropriate scaling factors. We find that $g_\parallel$ decreases from unity to 0.7 for C7 and 0.5 for C9, whereas $g_\perp$ grows from unity to 1.4 for C7 and up to 3 for C9. The theoretical evaluation of the anisotropic g requires a detailed microscopic model. One model approach [17] is to assume $S = 1$ so that the molecules are constrained to be parallel or antiparallel to the director axis. If the electric dipole lies at an angle β with respect to the long molecular axis, the anisotropic dipole-dipole correlation factors can be

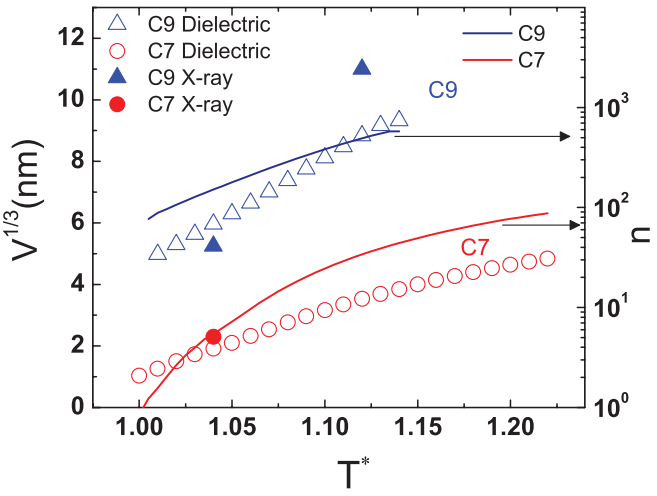

FIG. 6. (Color online) Cluster size $L = V^{1/3}$ compared to the x-ray scattering results $V^{1/3} = (\pi/6L_{\parallel}L_{\perp}^2)^{1/3}$ ($L_{\parallel}$ and $L_{\perp}$ from Ref. [3]) and the line represents n, the number of interacting molecules as a function of reduced temperature ($T^* = T_{N\text{-}I}/T$).

written as

$$g_{\parallel} = 1 - \frac{n\mu^2 \cos^2 \beta \left\langle 3\left(\frac{r_z}{r}\right)^2 - 1 \right\rangle}{4\pi\epsilon_o r^3 k_B T}, \tag{3}$$

$$g_{\perp} = 1 - \frac{n\mu^2 \sin^2 \beta \left\langle 3\left(\frac{r_x}{r}\right)^2 - 1 \right\rangle}{8\pi\epsilon_o r^3 k_B T}. \tag{4}$$

n is the number of neighbors. For a smectic order, the average separation perpendicular to the layers $r_z \gg$ in-plane separation, and this results in $g_{\parallel} < 1$. If $\langle r_x^2 \rangle < \langle r^2/3 \rangle$, we get $g_{\perp} > 1$, indicating a parallel alignment of the polar axes. On using the experimental values of $g_{\perp}$ and using Eq. (4), we calculate n for a smecticlike order. The average separation values perpendicular r_z and parallel r_x to the individual molecules are taken from the x-ray small-angle scattering and wide-angle peak positions [3], respectively. We note from Fig. 6 that n is increasing almost exponentially with T^*.

The effective volume V of the correlated molecules is estimated by multiplying n by the volume of a single molecule calculated from the molecular weight and density. The polar correlation lengths $l = V^{1/3}$ for C7 and C9 are shown in Fig. 6. It is interesting to compare the above findings with results from structural analysis obtained by x-ray scattering [14]. Results agree for C7 and C9 close to the I-N transition temperature. However, the structural correlation length increases (seen for C9) more rapidly than the polar one. In the structural analysis so far, the splitting in small-angle x-ray diffraction patterns has not yet been considered. The interpretation, in terms of the tilt of the SmC-type nanoclusters, from a strong temperature dependence of splitting for both C7 and C9, is more reasonable than that based on the form factor. The association found from the dielectric results provides information about the polar interactions, whereas from x-ray scattering it depends on the size and nature of the cluster, and the results from the two are in broad agreement with each other.

We studied three bent-core liquid crystals (C4, C7, and C9) with the same mesogenic core but with different terminal groups. These show different dielectric and small-angle x-ray scattering results. C4 with short terminal groups shows a change in the sign in $\Delta\epsilon'$ as a function of temperature and frequency in its nematic phase. C9 with long tails shows negative $\Delta\epsilon'$ in the entire nematic range. The behavior of C7 is intermediate of the two. The temperature dependencies of permittivity are related to a change in the strong anisotropic correlations among the molecules. Interestingly, for C9, we find a large kink in the $\epsilon_{\perp}$ and a small kink in $\epsilon_{\parallel}$ at the $N_{\text{cyb}C}$-Cyb$C$ transition [Fig. 5(c)]. This shows that clusters in $N_{\text{cyb}C}$ and Cyb$C$ phases behave differently. In the Cyb$C$ phase the macroscopic dipole of larger clusters tends to form a twisted structure to reduce the free energy, whereas in the $N_{\text{cyb}C}$, dipoles of individual clusters are arranged randomly [21].

This work was funded by EU FP7BIND (216025) and SFI 06/RFP/ENE039. A.K. thanks the Polish Scientific Committee for Grant No. N202282734.

[1] H. Takezoe and Y. Takanishi, Jpn. J. Appl. Phys. **45**, 597 (2006).
[2] R. A. Reddy and C. Tschierske, J. Mater. Chem. **16**, 907 (2006).
[3] C. Keith, A. Lehmann, U. Baumeister, M. Prehm, and C. Tschierske, Soft Matter **6**, 1704 (2010).
[4] J. Harden, B. Mbanga, N. Eber, K. Fodor-Csorba, S. Sprunt, J. T. Gleeson, and A. Jakli, Phys. Rev. Lett. **97**, 157802 (2006).
[5] D. B. Wiant, J. T. Gleeson, N. Eber, K. Fodor-Csorba, A. Jakli, and T. Toth-Katona, Phys. Rev. E **72**, 041712 (2005).
[6] B. R. Acharya, A. Primak, and S. Kumar, Phys. Rev. Lett. **92**, 145506 (2004).
[7] N. Vaupotic, J. Szydlowska, M. Salamonczyk, A. Kovarova, J. Svoboda, M. Osipov, D. Pociecha, and E. Gorecka, Phys. Rev. E **80**, 030701 (2009).
[8] O. Francescangeli and E. Samulski, Soft Matter **6**, 2413 (2010).
[9] O. Francescangeli, F. Vita, C. Ferrero, T. Dingemans, and E. T. Samulski, Soft Matter **7**, 895 (2011).
[10] V. Prasad, S.-W. Kang, K. A. Suresh, L. Joshi, Q. Wang, and S. Kumar, J. Am. Chem. Soc. **127**, 17224 (2005).
[11] B. R. Acharya, S.-W. Kang, and S. Kumar, Liq. Cryst. **35**, 109 (2008).
[12] C. Tschierske and D. J. Photinos J. Mater. Chem. **20**, 4263 (2010).
[13] Y. Jang, V. P. Panov, J. K. Vij, A. Lehmann, and C. Tschierske, Appl. Phys. Lett. **97**, 152903 (2010); A. Kocot, H. Xu, S. T. MacLughadha, and J. K. Vij, Mol. Cryst. Liq. Cryst. **261**, 501 (1995).
[14] H. Toriyama, S. Sugimari, K. Moriya, D. A. Dunmur, and R. Hanson, J. Phys. Chem. **100**, 307 (1996).
[15] H. Xu, J. K. Vij, A. Rappaport, and N. A. Clark, Phys. Rev. Lett. **79**, 249 (1997).

[16] W. T. Coffey and Yu. P. Kalmykov, Adv. Chem. Phys. **113**, 487 (2000).

[17] W. H. de Jeu, W. J. A. Goossens, and P. Bordewijk, J. Chem. Phys. **61**, 1985 (1974).

[18] P. Salamon, N. Eber, A. Buka, J. T. Gleeson, S. Sprunt, and A. Jakli, Phys. Rev. E **81**, 031711 (2010).

[19] H. G. Yoon, S.-W. Kang, R. Y. Dong, A. Marini, K. A. Suresh, M. Srinivasarao, and S. Kumar, Phys. Rev. E **81**, 051706 (2010).

[20] M. Stocchero, A. Ferrarini, G. J. Moro, D. A. Dunmur, and G. R. Luckhurst, J. Chem. Phys. **121**, 8079 (2004).

[21] S. D. Peroukidis, A. G. Vanakaras, and D. J. Photinos, Phys. Rev. E **84**, 010702(R) (2011).